Precambrian Research 438 (2026) 108064

Contents lists available at ScienceDirect

Precambrian Research

journal homepage: www.elsevier.com/locate/precamres

Reevaluating the nutrient timeline: Francevillian basin geochemistry reveals early permissive conditions for eukaryotic life

Anna El Khoury [a,b], Ernest Chi Fru [c], Ibtissam Chraiki [a], Mathias Harzhauser [d], Christian Aupissy [a], Claude Fontaine [a], Andrea Somogyi [b], Abderrazak El Albani [a,*]

[a] Université de Poitiers, IC2MP, UMR 7285, CNRS, 86073 Poitiers, France
[b] NANOSCOPIUM beamline, Synchrotron SOLEIL, 91190 Saint-Aubin, France
[c] Cardiff University, School of Earth and Ocean Sciences, CF10 3AT Cardiff, United Kingdom
[d] Natural History Museum Vienna, Geological-Palaeontological Department, Burgring 7, 1010 Vienna, Austria

A B S T R A C T

Environmental thresholds of oxygen and nutrients have played a pivotal role in shaping the timing and nature of major biological transitions throughout Earth's history. Limited marine phosphate availability is thought to have constrained the tempo and trajectory of early eukaryotic evolution. A sustained global rise in marine P and trace metal nutrient availability, reaching near-modern levels, coincided with the Neoproterozoic Oxidation Event (NOE) and the emergence and radiation of Ediacaran and Cambrian animal lineages. Here, we present new geochemical evidence from the 2.1-billion-year-old (Ga) Francevillian Basin that reveals a striking exception to this timeline. Our data indicate that Paleoproterozoic seawater in the Francevillian Basin episodically reached nutrient and oxygen levels comparable to, and in the case of phosphate and zinc, potentially exceeded concentrations associated with the seawater in which the Cambrian biota of Burgess Shale emerged. The data suggest that permissible key chemical conditions for complex life existed in the Francevillian sea long before the Ediacaran–Cambrian nutrient surge. The coincidence of this anomalous Paleoproterozoic nutrient-rich window with the earliest known marine experimentation at macrobiological complexity, represented by the much-debated 2.1 Ga Francevillian macrobiota, challenges established timelines of biological innovation and environmental prerequisites.

1. Introduction

A series of irreversible transitions are often linked to a progressive increase in biological complexity, diversification and resilience throughout Earth's history. These milestones are closely tied to the onset of global-scale stable plate tectonics (Korenaga, 2013), continental growth (Lee et al., 2016) and episodic Snowball Earth glaciations (Hoffman et al., 2017), which together transformed Earth's surface and modulated Proterozoic seawater nutrient content (Alcott et al., 2022; Chi Fru et al., 2024, 2023; Reinhard et al., 2017; Stüeken et al., 2016). These conditions boosted cyanobacterial activity, enabling permanent oxygenation of the atmosphere during the Great Oxidation Event (GOE) ~ 2.45–2.2 billion years ago (Ga) and the ~ 0.8–0.540 Ga Neoproterozoic Oxidation Event (NOE), and to the eventual emergence of eukaryotes and complex multicellular life (Brocks et al., 2017; Lyons et al., 2014, 2024; Poulton et al., 2021; Sumner, 2024).

Among the key biological innovations following the GOE is the emergence of the very much debated 2.1 Ga Francevillian Biota in Gabon (El Albani et al., 2010; Ikouanga et al., 2024), one of Earth's earliest known and morphologically diverse assemblages of macrofossils displaying complex properties associated with more advanced eukaryotic life forms (Chi Fru et al., 2024; El Albani et al., 2014, 2019, 2023; El Khoury et al., 2025c, 2025b; Ikouanga et al., 2023; Ossa Ossa et al., 2023). This discovery is both exceptional and problematic within the Paleoproterozoic context, a period of change characterized by widespread seawater anoxia and nutrient-poor oceans inhospitable to the energetic demands of a complex oxygen-respiring lifestyle. It challenges the prevailing view that eukaryotes first emerged ~ 1.8–1.6 Ga and that large morphologically and architecturally complex multicellular forms only evolved following a global supply of nutrients to the oceans by the melting Neoproterozoic Snowball Earth glaciations, ~720–635 million years ago (Ma) (Brocks et al., 2017; Chi Fru et al., 2023; Reinhard et al., 2017). These conditions are thought to have initiated sustained widespread oxygenation of the Neoproterozoic ocean–atmosphere system, priming the stage for the emergence of the ~635-541 Ma Ediacaran biota (Narbonne, 2005) and the ~ 541–485 Ma Cambrian explosion of the major groups of modern animals (Marshall, 2006).

Similar to the Francevillian Basin, the Ediacaran-Cambrian biota rose on the heels of significant environmental change, including fluctuations in sea levels and ocean chemistry (Babcock et al., 2015; Pruss

* Corresponding author.
E-mail address: abder.albani@univ-poitiers.fr (A. El Albani).

https://doi.org/10.1016/j.precamres.2026.108064
Received 5 November 2025; Received in revised form 19 February 2026; Accepted 23 February 2026
Available online 7 March 2026

and Gill, 2024), coupled to a greenhouse stable state, increases in seawater phosphorus content (Chi Fru et al., 2024; Reinhard et al., 2017) and a rise in atmospheric oxygen levels (Canfield et al., 2007; Lyons et al., 2014; Och and Shields-Zhou, 2012; Poulton et al., 2021). These changes suggest a causal relationship linked to a change to more permissive environmental conditions, higher nutrient and oxidant availability to satisfy the metabolic needs of larger and more complex organisms (Jiang et al., 2022). For example, complex multicellular life requires a stable redox regime with persistent oxygenation, nutrient-rich conditions, particularly increased P and N availability and access to essential trace elements. Currently, it is thought that these conditions first coalesced during the Neoproterozoic, ~1.0–0.541 Ga. Here we test the emerging suggestion that unique localized threshold conditions for complex multicellular life may have been met much earlier in the Francevillian Basin, ~2.1 Ga.

Unlike the global-scale terminal Neoproterozoic biotic transition, the Francevillian biota represents a localized episode of diversification in a restricted intra-cratonic basin isolated from the global ocean. This spatial isolation, combined with geochemical evidence for freshwater-influenced conditions rather than a fully marine environment (El Khoury et al., 2025a), limits direct stratigraphic correlations with other past marine records, posing challenges for testing evolutionary hypotheses relevant to the Francevillian window. However, the marked temporal and biological gap between the well-preserved fossil-rich Paleoproterozoic Francevillian and the Cambrian Burgess Shales provides a unique opportunity to constrain the environmental threshold controls on early complex life and assess whether conditions in the Francevillian Basin could have supported and sustained significant biodiversification. To explore this idea, we conducted a detailed comparative geochemical analysis of the Francevillian black shales to reconstruct seawater nutrient and oxygen dynamics and then compared observations with data from the Burgess Shale as a lower threshold baseline, the latter preserving exquisite details of soft-bodied oxygen-respiring ancestors of modern animal lineages (Anderson et al., 2021; Ma et al., 2015; Morris, 1989; Orr et al., 1998). Our findings suggest that, like the Cambrian seas, the Francevillian marine environment met key environmental nutrient thresholds and redox conditions to support a multicellular lifestyle, making it Earth's earliest cradle of complex life.

2. Geological setting

The Francevillian basin formed during the Paleoproterozoic, ~2.1 Ga (Ikouanga et al., 2024), is located in the Republic of Gabon in western equatorial Africa. This basin consists of several lithostratigraphic formations, designated as Francevillian (F) FA to FE, which rest unconformably on Archean basement rocks (Weber, 1968). The studied rocks come from the Moulendé quarry and are suitable for our study because they have been subject to only minimal tectonic deformation and show no evidence of metamorphic alteration (Bankole et al., 2015; Gauthier-Lafaye et al., 1996; Ikouanga et al., 2023; Ngombi-Pemba et al., 2014). The FA Formation primarily comprises fluviatile and deltaic sandstones but also contains mudstone (Bankole et al., 2020). At its top, it contains uranium enrichments and the notable Oklo natural nuclear reactors (Gauthier-Lafaye and Weber, 1989). The FB Formation is composed mainly of marine sediments deposited below storm wave base and is further subdivided lithologically into the FB1 and FB2 members, further divided into the FB1a-c and FB2a-c units, respectively. In this scheme, the FB1a-b units consist of interlayered shales, sandstones, and conglomerates that transition into predominantly shales at the top, while the FB1c unit consists primarily of shales, with a thin iron formation overlain by black shales and a manganese-rich interval. The FB2a unit includes sandstone beds deposited during sea level fall (Reynaud et al., 2018). This unit is sharply overlain by the FB2b unit, characterized by finely laminated black shales interbedded with thin siltstone layers deposited by waning storm surges. This unit contains remarkable specimens that are completely to partially pyritized and non-pyritized macrofossils found abundantly in the black shales (El Albani et al., 2019, 2014, 2010). The fossil abundance decreases towards the top of the section, where silty and sandy beds are more common. In the fossiliferous quarry, the FB2b black shales are 5 m thick and were deposited in a quiet, low-energy marine environment from a fully oxygenated water column (Canfield et al., 2013). The FC Formation is dominated by dolomites and stromatolitic cherts, indicative of shallow-water depositional conditions. Stromatolites are found on topographic highs at its base (Bertrand-Sarfati and Potin, 1994). Finally, the FD Formation corresponds to black shales deposited during a transgressive phase, while the FE Formation has been predominantly eroded across the basin. For complete geological background including maps, stratigraphic schemes and detailed profiles of the quarry, kindly refer to Aubineau et al., (2018); Canfield et al., (2013); Reynaud et al., (2018).

The Walcott Quarry Burgess Shale, located in the Canadian Rocky Mountains of British Columbia, is part of the Middle Cambrian Stephen Formation (~508 Ma). It lies at the base of the Yoho Group and is overlain by carbonate rocks of the Eldon Formation (Collins et al., 1983). It was originally deposited on the western margin of Laurentia along a passive continental margin, which was then deformed by the Laramide Orogeny, forming the present mountainous setting (Liu et al., 2010). It is a succession composed of calcareous, silt-bearing mudstones interbedded with limestones (Fletcher and Collins, 1998). The Burgess Shale was deposited on the slope of an ancient underwater escarpment known as the Cathedral Escarpment, a steep drop-off from a carbonate reef platform into a deep basin (Stewart et al., 1993). Rapid cyclic mudflows buried organisms quickly (Collom et al., 2009), leading to exceptional preservation of diverse soft-bodied organisms all lying within the shale basin adjacent to the Cathedral and Eldon escarpments, making this site one of the most important Lagerstätte on Earth (Morris, 1989). These fossils deposited under oxic conditions despite the presence of localized anoxic environments along the base of the Cathedral Escarpment (Powell et al., 2003). For more detailed geological and stratigraphical background, kindly refer to Anderson et al., (2024); Bottjer, (2002); Caron et al., (2014); Caron and Jackson, (2008).

3. Materials and methods

Thirty-five representative bulk sediments were sampled (15 from sediments collected adjacent to fossil specimens in the Walcott Burgess Shales and 20 from the Francevillian FB2b black shales). Because of restricted access to the Walcott quarry itself, the acquisition of such reference material is consequently rare. Therefore, the analyses are based on well-curated reference material collected from the original fossil-bearing layers and housed at the Natural History Museum, Vienna. The samples were powdered with an agate mortar. Mineralogical composition of bulk and clay fraction was investigated by X-Ray diffraction (XRD) using a Bruker D8 ADVANCE diffractometer at the University of Poitiers, France (voltage 40 kV, probe current 40 mA, time per step 1 s, step 0.2) for an angular range of 2–65° 2θ and 2–35° 2θ for bulk and clay fraction, respectively. The dispersion of the powder in deionized water with an Elma S60 ultrasonic agitation device without any chemical pretreatment allowed the recovery of < 2 μm clay fraction by sedimentation (Moore and Reynolds, 1997). Oriented preparations of the < 2 μm size fraction were prepared by drying a ~ 1 mL suspension on glass slides at room temperature. The oriented mounts were examined after successive air-dried (AD) and ethylene glycol (EG) saturation. X'Pert Highscore software was used for background stripping, indexing of XRD peaks and mineral identification by comparing with International Centre for Diffraction Data (ICDD) files.

Geochemical analyses on the 35 samples were undertaken at the Service d'Analyse des Roches et Minéraux (SARM), Centre de Recherches Pétrographiques et Géochimiques (CRPG) in Nancy, France. Approximately 1 g of powdered sample was fused with lithium metaborate ($LiBO_2$) and dissolved in dilute nitric acid (HNO_3). Major

and trace elements data were obtained using Inductively Coupled Plasma Atomic Emission Spectrometry (ICP-AES) while rare earth elements (REE) were obtained using Inductively Coupled Plasma Mass Spectrometry (ICP-MS) following the techniques described in Carignan et al. (2001). Information about the method of calculation of Ce and Eu anomalies, enrichment factors, and chemical index of alteration and weathering can be found in the supplementary file (Supplementary Material). TOC analyses were performed using the Rock-Eval 6 Turbo device at Sorbonne University, operating in an adapted method for sedimentary rocks (Bulk Rock/Basic (Behar et al., 2001). Pearson

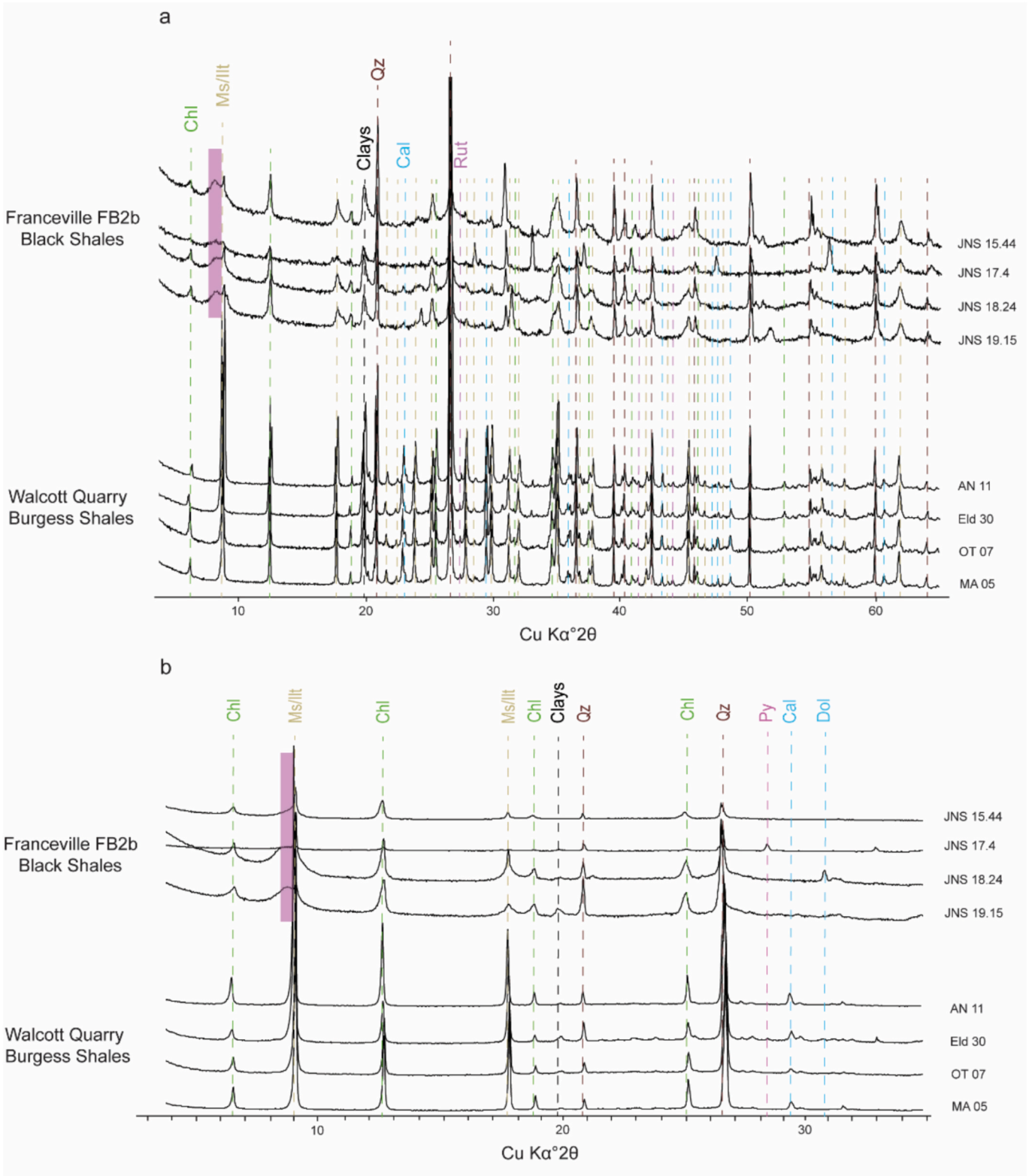

Fig. 1. Mineralogical composition of the Franceville and Walcott Quarry deposits. a, Bulk XRD mineralogy and b, Clay fraction analyses of the two deposits showing a broadly similar mineralogical and major clay composition.

correlations and *t*-test analyses were carried out using PAST statistical software.

4. Results and discussion

Mineralogical Comparisons Between Francevillian FB2b and Burgess Shale

Comparative bulk mineralogical study of the Francevillian FB2b unit and the Walcott Burgess Shale deposits suggests major elemental, mineralogical and sedimentological similarities. Both are primarily composed of quartz, illite/muscovite and chlorite with occasional occurrences of carbonate minerals (dolomite, calcite, ankerite) and pyrite (Fig. 1a). The Burgess Shales contain traces of rutile and K-feldspars, whereas these minerals are absent in the Gabonese unit. The presence of rutile and feldspar in the Burgess Shale and absence in Franceville is consistent with reconstructed weaker and stronger chemical weathering of their source rocks, respectively (Fig. 2a-b). In fact, while feldspars are readily altered during chemical weathering, their preservation generally indicates limited weathering intensity (Fedo, 1995; Nesbitt and Young, 1982; Taylor and McLennan, 1985). Clay mineralogical analysis confirms the dominance of illite and/or mica and chlorite in both deposits (Fig. 1b), with higher abundance and crystallinity of illite/mica in Burgess. While the Burgess shales lack swelling clays, the FB2b Francevillian Formation contains smectite-rich randomly ordered mixed layers due to incomplete illitization reaction because of potassium deficiency, particularly K-feldspars (Aubineau et al., 2019; Ngombi-Pemba et al., 2014). Kaolinite is absent in both deposits (Anderson et al., 2021; Ngombi-Pemba et al., 2014).

Provenance and Post-depositional Overprinting of Geochemical Signatures

La-Th-Sc and Th/Co vs La/Sc diagrams indicate a felsic source, clustering in the intermediate TTG field for both localities (Fig. 2c-d), consistent with previous studies for Franceville (Bankole et al., 2020). TOC values for the Francevillian FB2b unit yield values ranging from

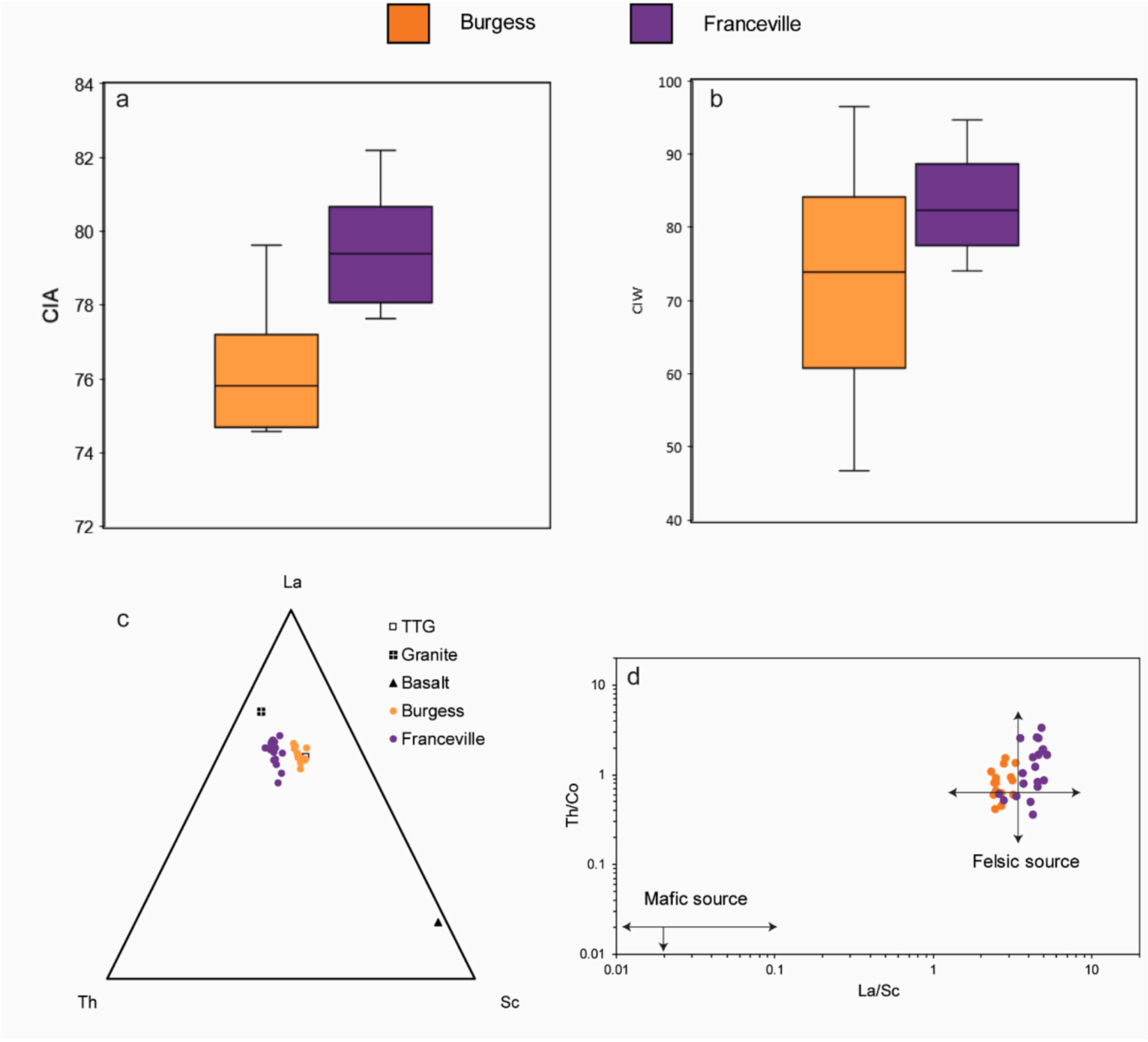

Fig. 2. Chemical weathering and provenance. a, Chemical index of alteration (CIA) and b, chemical index of weathering (CIW) suggest a higher intensity of weathering for the Francevillian deposits compared to Burgess Shales. c, La-Th-Sc plot and d, Th/Co vs La/Sc plots suggest a felsic TTG source for both deposits.

0.17-3.19 wt%, with a mean of 1.05 wt% (Table S1). Organic carbon values for the Burgess Shale yield similar values as presented in Powell (2009), ranging from 0.14 to 2.42 wt%. Exceptional soft-tissue preservation in the Burgess Shale and, to some extent, in Franceville, implies fine-grained clay minerals and carbon films were not recrystallized beyond recognition. Illite crystallinity and mineral assemblages indicate very low-grade metamorphic temperatures for Burgess Shale, much lower than would obliterate sedimentary textures (Fig. 1). Moreover, the Francevillian FB2b deposit is known for its exquisite preservation and lack of metamorphic overprinting (El Khoury et al., 2025b; Ikouanga et al., 2023; Ngombi-Pemba et al., 2014). Thus, both successions are considered low-grade metamorphosed, preserving primary sedimentary fabrics and fossil outlines. In geochemical terms, this implies that trace and rare earth element (REE) patterns can still be considered reliable for paleoenvironmental interpretation (Lawrence et al., 2006).

Paleoclimatic Depositional Conditions

Chemical weathering on the continents is assumed to be primarily constrained by variations in atmospheric temperature and humidity; thus, the intensity of chemical weathering in sediments can aid in paleoclimate reconstruction (Sun et al., 2022; Wang et al., 2020). In arid and polar climates, chemical weathering intensity is commonly weak due to cold temperatures and limited precipitation, while physical or mechanical erosion, for example, is more prevalent, resulting in no real change in the chemical composition of the parent rock (Nesbitt and Zipser, 2003). On another hand, in warmer and wetter environmental conditions, chemical reactions happen between the parent rock and a solvent, which results in selective removal of mobile cations, and therefore the production of a chemical composition of rocks different from the parent rock. This phenomenon is characterized by high CIA and CIW values. CIA values of Burgess and Franceville sediments (average 76.25 and 79.55, respectively), also supported by CIW values (74.37 and 81.89, respectively) indicate intermediate to high chemical alteration, characteristic of a temperate climate for samples from the Walcott Quarry, while those of Gabon suggest a warmer environment (Fig. 2a-b) (Fedo, 1995; Harnois, 1988). As we show subsequently, this high chemical weathering likely released significant amounts of nutrients from felsic source rocks, enriching seawater and supporting vigorous primary productivity.

REE Comparisons Between Francevillian FB2b and Burgess Shale

Burgess shales show higher REE enrichment compared to the Francevillian shales (Table S2). PAAS-normalized REE + Y spectra (Lentz, 2003) display a flat pattern with a slight light REE (LREE) (La-Sm) enrichment and general Heavy REE (HREE) (Er-Lu) depletion in both deposits (Fig. 3 a-b). Eu anomalies (Eu/Eu*) range from 1.04 to 2.66 for the Burgess Shale and 0.77–1.28 for the FB2b unit (Table S2). While strong positive Eu anomaly often supports high-temperature hydrothermal fluxes to the water column (Planavsky et al., 2010), the Fe/Ti versus Al/(Al + Fe + Mn) hydrothermal proxy (Boström, 1970) indicates stronger detrital rather than active hydrothermal enrichment (Fig. 3c), consistent with previous observations (Aubineau et al., 2020; El Khoury et al., 2025c). Despite the observed Eu anomaly, the fossil-bearing FB2b unit examined in this study does not display geochemical signatures indicative of contemporaneous submarine volcanic or hydrothermal activity. Rather, submarine volcanic activity is most pronounced during deposition of the stratigraphically underlying unit (Chi Fru et al., 2024). For example, Fe/Ti versus Al/(Al + Fe + Mn) ratios for FB2b samples do not cluster within the active hydrothermal field (Fig. 3c), whereas samples from the underlying unit do (Chi Fru et al., 2024). The relatively

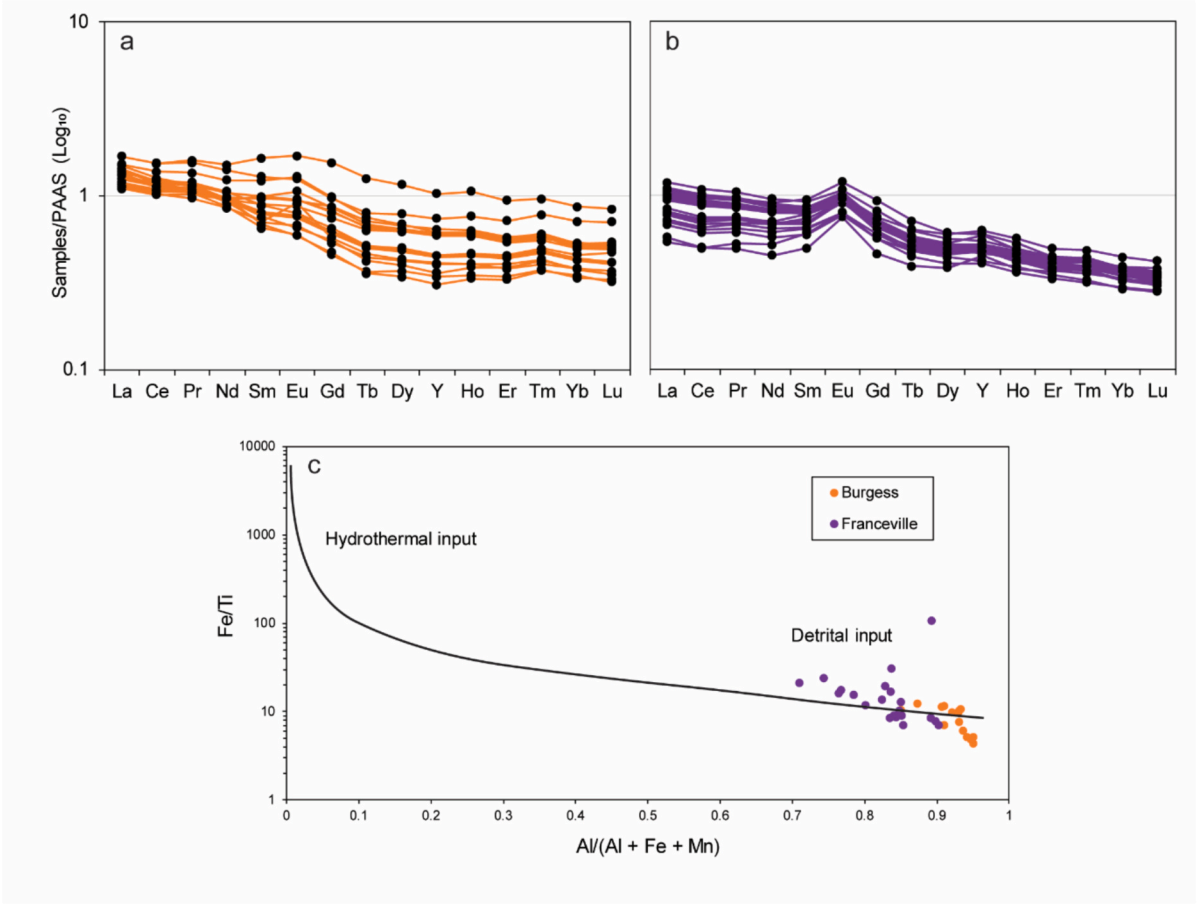

Fig. 3. Geochemistry of the studied samples. PAAS-normalized REE + Y patterns of a, Burgess Shales and b, Francevillian black shales. PAAS values are from (Lentz, 2003). c, Binary plot of Fe/Ti vs Al/(Al + Fe + Mn) after (Pecoits et al., 2009).

high Al/(Al + Fe + Mn) ratios and low Fe/Ti values observed in FB2b are instead consistent with a dominant detrital sedimentary input. These characteristics are most parsimoniously explained by recycling of material related to the underlying hydrothermally influenced succession, during which Fe and Mn were preferentially depleted, coupled to enrichment of Al and retention of primary Eu anomalies. This interpretation is further supported by an up-section increase in the chemical weathering, suggesting enhanced weathering of source materials during FB2b deposition (Chi Fru et al., 2024; El Khoury et al., 2025c). The Burgess Shale samples similarly do not plot within the active hydrothermal field, instead clustering in the detrital field, with their Fe/Ti and Al/(Al + Fe + Mn) ratios being broadly comparable to those observed in the Francevillian FB2b subunit. Together with the presence of a weak Eu anomaly, the above observations suggest broadly analogous depositional processes during the accumulation of the Burgess Shale, with only subtle geochemical differences (Fig. 3).

Geochemical Classification from Major Oxides

Log(Fe_2O_3/K_2O) vs log(SiO_2/Al_2O_3) ratios (Herron, 1988) classify most of the samples as shale (Fig. 4) by differentiating them based on their major oxide composition. The clustering of samples within the shale field indicates fine-grained sediments dominated by low-Fe aluminosilicate clays and mica, consistent with our mineralogical data (Fig. 1) and previous analysis (Anderson et al., 2021; Aubineau et al., 2019; Ngombi-Pemba et al., 2014). The Fe_2O_3/K_2O ratio captures the relative input of iron oxides vs potassium-bearing minerals such as feldspars and micas, which are sensitive to mineralogical, provenance and diagenetic alteration, and the SiO_2/Al_2O_3 ratio the relative abundance of quartz to aluminosilicate minerals, interpreted as a proxy for weathering intensity and sediment maturity. The low SiO_2/Al_2O_3 indicate minimal reworking and deposition in a proximal, low-energy depositional setting fed predominantly by felsic to intermediate source rocks (Fig. 4).

Element Correlation Patterns and Mineral Associations

The major elements in the Franceville sediments, normalized to Post Archean Australian Shale (PAAS) (Lentz, 2003), show a slight enrichment in SiO_2 and P_2O_5 (EF > 1), while being depleted (EF < 1) in the Burgess Shale (Fig. 5; Table S3). Both sites are depleted in Fe_2O_3, Na_2O and TiO_2. The Francevillian sediments are remarkably enriched in MnO and MgO compared to the Burgess Shale, which is slightly more enriched in CaO and K_2O, potentially indicating a higher carbonate, mica and feldspars content. Overall, the Francevillian basin is enriched in all major elements analyzed, except CaO, K_2O and TiO_2, which show slight

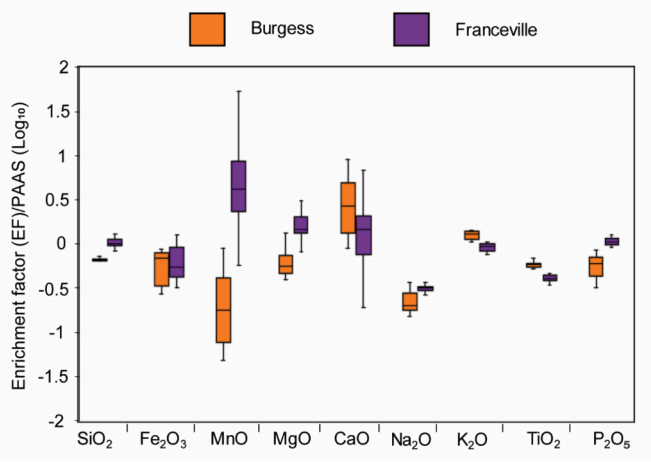

Fig. 5. Major elements enrichment factor (EF) relative to PAAS in Burgess and Franceville samples.

relative enrichment in the Burgess Shale (Fig. 5), in agreement with the presence of carbonates, feldspars and rutile in the latter (Fig. 1).

SiO_2 is not positively correlated to any major element in the Franceville samples, suggesting decoupling between quartz and the clay-rich fraction. This pattern is consistent with selective chemical weathering of the source rocks, whereby labile silicate minerals were preferentially altered to clay minerals, while chemically resistant quartz was preserved as a detrital or residual phase that behaves independently of the bulk clay mineral matrix (Tables S4, S5; Figs. S1, S2) (Nesbitt and Young, 1982; Taylor and McLennan, 1985). On the other hand, a positive correlation with Al_2O_3 and TiO_2 in the Burgess Shale suggests that SiO_2 is not present solely as detrital quartz but may be partially associated with fine-grained heavy minerals or clay-sized accessory phases (Tables S4, S5; Figs. S1, S2). This observation is consistent with greater enrichment of TiO_2 in the Burgess Shale compared to Franceville, while a positive correlation of Al_2O_3 with Na_2O and K_2O supports association with clay minerals. The lack of correlation between MnO and major elements in the Francevillian unit is consistent with authigenic chemical precipitation of manganese oxides and carbonates from seawater in Franceville (Mayika et al., 2020). This is also consistent with the MgO and CaO being positively correlated, pointing to the presence of dolomite and carbonates. P_2O_5 correlates with Al_2O_3 and TiO_2 in the FB2b

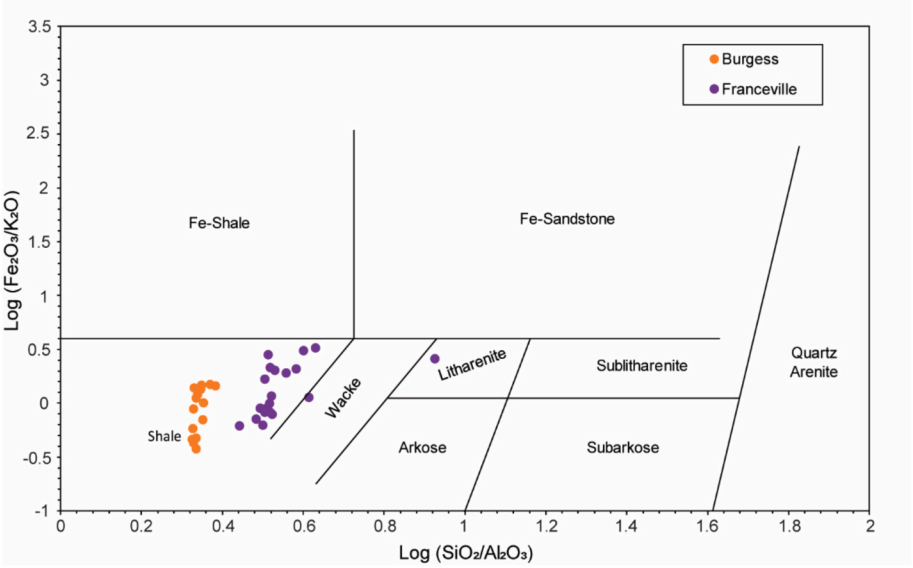

Fig. 4. Rock classification of samples using Herron's diagram. Most of the samples cluster in the shale domain.

Francevillian unit, indicating a strong detrital contribution (Tables S4, S5; Figs. S1, S2). Correlation between MgO and MnO in the Burgess Shales points to a likely brine-related origin (Powell, 2009), while the absence of correlation between Al_2O_5 and TiO_2 with P_2O_5 indicates negligible detrital influence. However, P/Ti and P/Al ratios suggest a stronger non-detrital P component is also present in Franceville compared to the Burgess Shale (Fig. 6 a-b). Overall, based on Fe/Al and Fe/Ti ratios, non-detrital Fe is more abundant in Franceville (Fig. 6 c-d).

Redox reconstruction

Fe/Al ratios indicate oxic conditions in both basins, corresponding

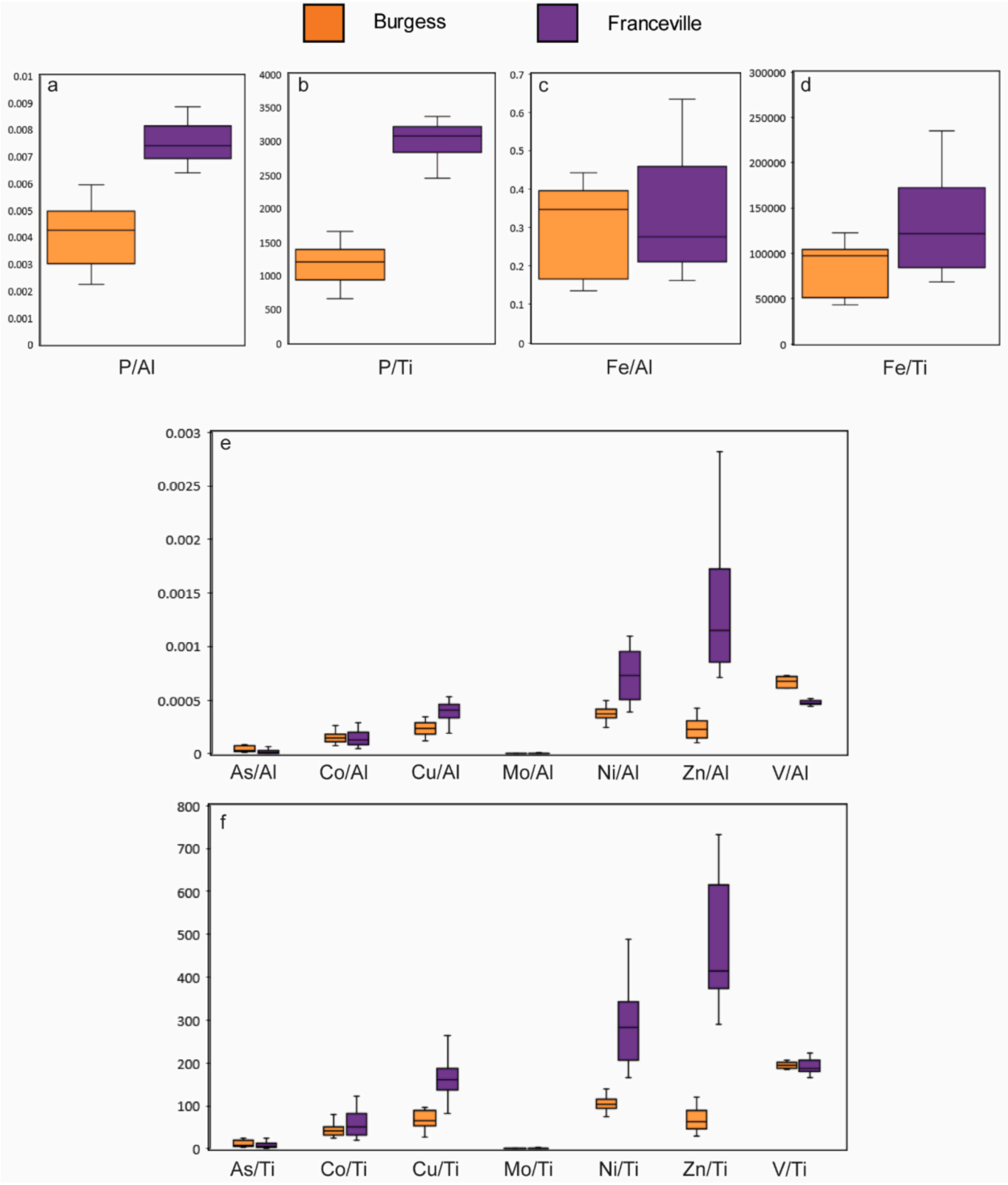

Fig. 6. Selected bio-essential elements correlation with Al and Ti for Burgess and Franceville samples.

with atmospheric oxygen levels above ~ 1% PAL, with slightly higher mean values in FB2b (0.34) compared to the Burgess Shale's 0.29 (Fig. 7a). U/Th ratios range from 0.09 to 0.17 in the Burgess Shale and 0.07–0.15 in FB2b, also suggesting oxic conditions, potentially with > 1–10% PAL O_2 (Fig. 7b). Ni/Co ratios are < 5 in the Burgess Shale, indicating oxic settings, whereas values of 5–7 in FB2b point to locally dysoxic conditions (Fig. 7c), consistent with independent findings for the Burgess Shale (Powell, 2009; Powell et al., 2003). Slightly negative Ce anomalies (Ce/Ce*) (Lawrence and Kamber, 2006) of ~ 0.92–0.94 in both units support broadly comparable O_2 levels in the two depositional settings (Fig. 7d).

Increasing Fe/Al ratios, reflecting high Fe^{2+} mobility, are common in anoxic or O_2-poor conditions (Lyons and Severmann, 2006; Clarkson et al., 2014; Raiswell et al., 2018). On the other hand, low Fe/Al ratios correlate with higher O_2 content, where Fe is oxidized to Fe^{3+} and precipitated or lost from solution (Lyons and Severmann, 2006; Raiswell et al., 2018). Because Al, a detrital element, remains largely unaffected by redox conditions, it normalizes the level of dissolved Fe input.

In addition, some redox-sensitive elements (e.g., Mo, Ag, Zn, Ni, Co, Cr V, U and Pt) have all been noted to be significantly enriched in modern muds and ancient black shale deposits (Calvert and Pedersen, 1993) and are used to unravel the paleo-redox conditions of depositional settings due to their distinct behaviors under different redox conditions (Tribovillard et al., 2006), thus allowing the identification of oxic, dysoxic, and anoxic depositional settings. Not all elements are equally reliable (Jones and Manning, 1994). Consequently, a series of metal ratios have been employed as redox proxy indicators, such as U/Th, V/Cr and Ni/Co (Kimura and Watanabe, 2001). Vanadium correlates positively with Al and thus could not be used as a redox proxy due to strong detrital influence (Fig. S3b-c). However, U/Th and Ni/Co are adequate ratios to be used in this case. Thorium (Th) is immobile and insoluble under all redox conditions and therefore reflects detrital input, while Uranium (U) is soluble in oxidized seawater (as U^{6+}) and precipitates under reducing conditions as U^{4+} (Bennett and Canfield, 2020). Thus, when bottom waters are anoxic, U is removed from seawater and concentrated in sediments, raising the U/Th ratio. On the other hand, under oxic conditions, U remains in solution, and U/Th in sediments stays low, reflecting crustal background ratios of ~ 0.26–0.3 (Bennett and Canfield, 2020). U/Th ratio values range from 0.09 to 0.17 for Burgess Shales and 0.07–0.15 for Franceville, with a mean of 0.12 and 0.08, respectively, suggesting broadly similar oxic conditions in both basins (Fig. 7b), with O_2 likely > 1–10% PAL (Marynowski et al., 2012).

Ni and Co are both redox-sensitive transition metals. Under reducing conditions, Ni is more mobile and more readily incorporated into organic-rich anoxic-O_2-poor sediments than Co. Under oxic-O_2-rich conditions, Co is more stable, and both elements are less enriched in sediments (Jones and Manning, 1994). Therefore, higher Ni/Co ratios generally indicate reducing anoxic environments, while lower ratios suggest oxidizing conditions. Although Ni/Co values might vary between the two depositional settings (Algeo and Liu, 2020; Jones and Manning, 1994), ratios > 5 correspond to strongly reducing-anoxic conditions marked by extremely low O_2 content and ratios of 5–1 are interpreted to reflect suboxic to weakly oxic conditions. Our Ni/Co ratio values are < 5 for the Burgess Shale, indicating an oxic environment (Fig. 7c). The Ni/Co ratios are generally higher for the FB2b unit with values clustering mainly in the dysoxic zone of 5–7 with a mean of 5.69 (Fig. 7c). We highlight that the Ni/Co proxy is empirical and context-dependent, with dissolved Ni and Co concentrations more strongly influenced by productivity and sedimentation rate that controls trace metal uptake by sediments (Algeo and Maynard, 2004; Liu and Algeo, 2020).

The Ce anomaly (Ce/Ce*) (Lawrence and Kamber, 2006) quantifies the deviation of Ce from expected REE behavior due to its unique redox sensitivity. Cerium can exist in both + 3 and + 4 oxidation states. In oxidizing conditions, Ce^{4+} precipitates from seawater, resulting in a negative Ce anomaly (Ce/Ce* <1). In anoxic conditions, Ce remains in the soluble Ce^{3+} form, and the anomaly is absent or positive, with Ce/Ce* equivalent to 1 or > 1. In our samples, Ce/Ce* values vary between 0.89 and 0.94 for the BS, with a mean of 0.92 and between 0.92 and 0.99, with a mean of 0.94 for the FB2b, indicating a slight negative Ce anomaly for both deposits (Fig. 7d; Table S2). The reliability of Ce/Ce* in shales depends on the balance between detrital (lithogenous) and authigenic (hydrogenous) REE inputs (Tostevin et al., 2016). In sediments dominated by detrital REEs, Ce/Ce* values typically reflect the crustal signature (≈0.9–1.0) and provide little redox information (Lawrence and Kamber, 2006). To evaluate this, correlations between

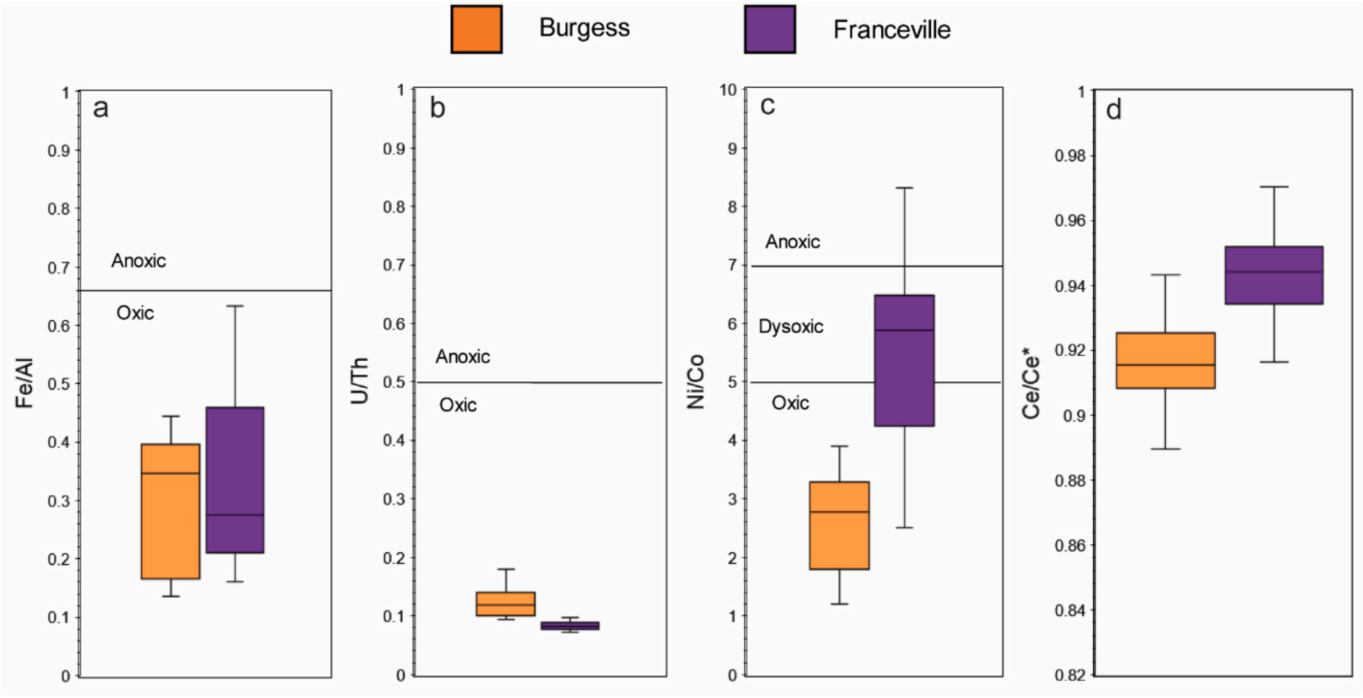

Fig. 7. Redox proxies showing redox depositional conditions. a, Fe/Al, b, U/Th, c, Ni/Co and d, Ce anomaly.

ΣREE, Ce and Ce/Ce* with Al and Ti as detrital proxies were examined (Fig. S6). In both basins, ΣREE correlates moderately with Ti (R^2 = 0.53–0.62) (Fig. S6a), suggesting that detrital phases modestly influenced total REE concentrations. A weak correlation with Al (R^2 = 0.08–0.39) in both localities further indicates limited control by clay and heavy mineral phases, and an alignment with authigenic enrichment (Fig. S6b). While Ce shows some correlation with Ti and to a lesser extent with Al (Fig. S6c, d), Ce/Ce* displays much weaker relationships (Fig. S6e, f), indicating partial decoupling from detrital sources and suggesting that Ce anomaly is not primarily governed by lithogenic input but reflects redox-dependent Ce oxidation during deposition.

On the other hand, observations were cross-validated with previous Fe speciation analyses (Canfield et al., 2013), which align with and support the redox interpretation. For example, FeHR/FeT ratios in the FB2b unit yielded values < 0.38, showing deposition beneath an oxygenated water column (Canfield et al., 2013). Moreover, FePy/FeHR ratio indicated values < 0.3, pointing to negligible euxinic depositional conditions (Canfield et al., 2013). These observations were also supported by the absence of U, Mo and V enrichments, indicating well-oxygenated bottom water conditions during deposition of the FB2b unit in Franceville (Canfield et al., 2013) and the shales of the Walcott Quarry (Powell et al., 2003). High organic matter content, together with rapid sedimentation, is reported in various instances in Franceville (Reynaud et al., 2018), with a high organic-carbon content in the FB2b black shales pointing to a highly productive shelf environment driven by cyanobacteria activity (Canfield et al., 2013).

These proxies provide further support for similar O_2 levels in both depositional settings (Tostevin et al., 2016), considering the similar bottom water oxygenation thresholds recorded in Franceville as in the Burgess Shale deposited at a time when atmospheric oxygenation levels were much higher than Paleoproterozoic estimates (Lyons et al., 2014, 2024).

Nutrient enrichment and biological implications

By ~ 2.1 Ga, the Congo Craton, to which the marginal Francevillian series was likely located at moderate latitudes within the emerging supercontinent Nuna/Columbia landmass (Salminen et al., 2016), though the exact coordinates are a subject of ongoing paleomagnetic and geological refinement. On the other hand, deposition of the Burgess Shale occurred in a paleogeographic tropical to low-latitude margin setting with ancient Laurentia, in an offshore, relatively deep marine environment (Scotese, 2021). Despite these contrasting depositional settings and ages, redox proxies indicate that both the Francevillian FB2b and Burgess Shales accumulated beneath dominantly oxic waters (Fig. 7). This shared redox framework allows nutrient enrichments, major and trace-metal cycling to be interpreted assuming similar redox baseline conditions. Differences in nutrient concentrations are therefore attributed to basin-specific controls on nutrient supply, retention, and dilution, rather than to differences in oxygenation. Moreover, it is important to note that bulk sediment enrichment factors and elemental ratios provide indirect constrains on past nutrient availability and cannot be directly equated with dissolved seawater concentrations. Processes such as early diagenetic retention, sediment focusing, basin-scale recycling and post-depositional redistribution may locally amplify nutrient concentrations within sediments. Accordingly, the following interpretations remain framed in terms of enhanced nutrient retention and availability within the basin system, particularly at the sediment–water interface.

Phosphorus (P) is enriched in FB2b (EF mean = 1.12) but depleted in Burgess (EF mean = 0.58) (Fig. 8; Table S3), with statistically significant differences (t-value = 5.85, 95% CI = (137, 284), p value = 1.49×10^6, critical t-value (for p = 0.05) = 2.0). Phosphorus is indispensable for all life forms. Considered to have limited primary production over Earth's history (Reinhard et al., 2017), P plays a crucial role in numerous biological processes. It is the backbone of nucleic acids, a key component of cell membrane phospholipids, and is essential for the synthesis and function of adenosine triphosphate (ATP) (Chi Fru et al., 2024, 2023; Laakso et al., 2020; Reinhard et al., 2017). Redox proxies indicate that bottom-water conditions during deposition of both successions were dominantly oxic. In such environments, Fe (oxyhydr)oxides commonly scavenge phosphorus (Bruland and Lohan, 2006). However, the absence of a correlation between P and Fe in both formations (Fig. S3a) suggests that Fe-bound scavenging was not the dominant control on phosphorus availability. In the FB2b unit, P correlates with Al and Ti (Table S4; Fig. S1), indicating a strong detrital component. However, P/Al and P/Ti ratios reveal significant authigenic P enrichment in Franceville compared to the Burgess Shale (Fig. 6a-b), suggesting that P was likely far more bioavailable in the Francevillian seawater. The restricted nature of the Francevillian Basin, coupled with tectonic activity associated with the ~ 2.1 Ga collision of the Congo–São Francisco cratons, likely promoted submarine volcanic weathering of nutrient-rich substrates, enriching the basin waters (Chi Fru et al., 2024). Following this volcanic input, basin restriction and early diagenetic exchange at the sediment–water interface could have facilitated efficient retention and recycling of phosphorus under oxic conditions, in line with recent models of Proterozoic phosphorus cycling (Guilbaud, 2025). These processes would have sustained elevated concentrations of bioavailable phosphorus relative to open-marine environments (Reinhard et al., 2017), supporting the interpretation of the Francevillian Basin as a localized Paleoproterozoic nutrient-rich oasis (Chi Fru et al., 2024). It has to be noted that the residence time of volcanically derived nutrients in a restricted intracratonic basin, and the duration over which such chemical modifications could persist in seawater remain difficult to constrain. However, limited water exchange and internal recycling may allow geochemical signatures introduced during earlier volcanic phases to be retained or reworked within the basin over extended intervals (Wang et al., 2024). Accordingly, the inferred linkage between earlier volcanic activity and nutrient enrichment in the FB2b unit is presented as a plausible basin-scale scenario consistent with stratigraphic and geochemical observations.

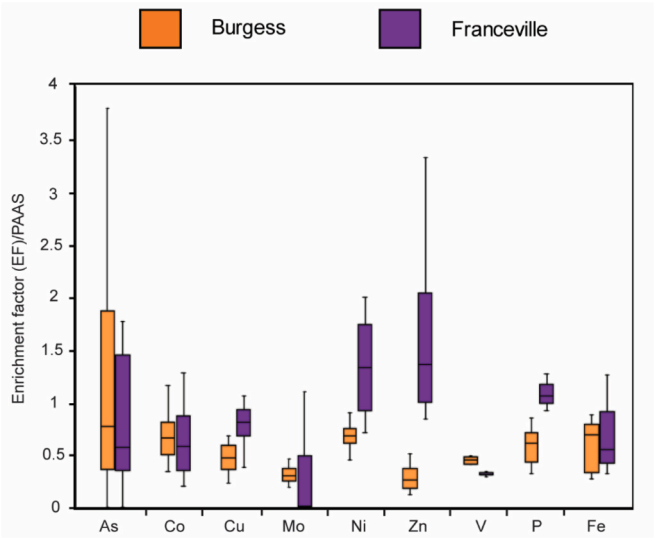

Fig. 8. Selected trace elements enrichment factor (EF) relative to PAAS for Burgess Shale and Franceville Black shales.

Toxic As, in the oxidized form of arsenate, disrupts phosphate uptake into cells, the synthesis of ATP and the functioning of membrane phospholipids (Chi Fru et al., 2019, 2018, 2016; Chraiki et al., 2023; Elias et al., 2012). Despite being less enriched in Franceville (mean of EF 1.44 versus 2.57 in Burgess Shales) (Fig. 8), the Gabonese macroorganisms detoxified As by sequestering within their bodies, similar to some of the more complex Burgess Shale biota (El Khoury et al., 2025c). Arsenate detoxification would have been critical considering a surge of arsenate in oxygenated Proterozoic seawater (Chi Fru et al., 2019), where these

organisms thrived. Within this framework, evidence for microbial mats, microbial sulfate reduction, iron and manganese cycling, primary production, and arsenic cycling has been reported from both settings (Aubineau et al., 2020, 2019, 2018; Caron and Jackson, 2008; Chi Fru et al., 2024; El Khoury et al., 2025c, 2025b; Gaines et al., 2008). While these biologically mediated processes may have influenced nutrient uptake and recycling at local scales, their net effect on basin-scale nutrient availability remains difficult to quantify. Nonetheless, our geochemical proxies indicate that dissolved nutrients, particularly phosphorus, were sufficiently available to support substantial biological activity. Any biologically driven modulation of nutrient and trace-element availability would likely have operated at the scale of individual communities or depositional environments (Falkowski et al., 2008) and remained secondary to basin-scale controls on nutrient supply, recycling efficiency, and long-term geochemical preservation.

Iron, a vital element involved in electron transport proteins (e.g., ferredoxin) (Arnon, 1965), the nitrogenase enzyme critical for nitrogen fixation, and other metabolic pathways essential for cell growth and respiration (Kustka et al., 2002), have mean EF values of 0.59 and 0.68 for the Burgess and Franceville shales, respectively (Fig. 8). Iron associates mainly with MgO and MnO (Tables S4, S5; Figs. S1, S2). Molybdenum, crucial for enzymes involved in nitrogen metabolism and cellular detoxification (Singh et al., 2017), is nearly absent in both sediments and shows no correlation with Al and Ti (EF mean = 0.36 and 0.21 for Burgess and Franceville, respectively) (Fig. 8; Tables S4, S5, Figs. S1, S2).

In the Gabonese FB2b unit, none of the selected trace elements correlates with Al or Ti, suggesting low detrital inheritance (Table S6; Fig. S4). However, As, Co, Cu, Mo and Ni are positively intercorrelated, while Zn appears to have a distinct source, uncorrelated with these elements. Dissimilar from Franceville, Cu and Zn content in the Burgess Shale correlate with Al and Ti, indicating a predominantly detrital origin (Table S7; Fig. S5) and therefore of lesser bioavailability, in addition to Zn being significantly more enriched in Franceville (EF = 1.53) compared to the Burgess Shales (mean EF = 0.36) by a factor > 4 (Fig. 8). Zinc is believed to be associated with organic matter and is strongly enriched in pyritized and non-pyritized macrofossils in the Francevillian biota (El Albani et al., 2023; Ossa Ossa et al., 2023). These elevated Zn concentrations and their associated negative Zn isotope signatures have been used to ascertain the eukaryotic origin of these enigmatic fossils (El Albani et al., 2023; Ossa Ossa et al., 2023). Being a bio-essential micronutrient, Zn is notable for its non-toxicity as Zn^{2+}, redox stability and strong affinity for various biologically relevant ligands (Weber et al., 2018), with eukaryotes having a much higher requirement compared to prokaryotes (El Albani et al., 2023). Cellular uptake is tightly regulated by proteins, enabling its diverse roles, ranging from enzymatic catalysis to structural functions in membranes, DNA and RNA function (Lim et al., 2005).

Overall, EFs calculated relative to the PAAS standard suggest most bioessential metals are depleted in both successions, except for Ni and Zn being notably more enriched in the Fb2b unit (Fig. 8). Mo, the cofactor critical for the functioning of nitrogenase enzymes used for nitrogen fixation (Darnajoux et al., 2019; Stüeken et al., 2016), shows a wider range in Franceville compared to Burgess. Ni, an important cofactor in anaerobic methane cycling (Glass and Orphan, 2012) and some higher life forms (Harasim et al., 2015), is enriched by ~ 2 times in the Francevillian FB2b unit (EF = 1.31) relative to the Burgess Shales (EF = 0.67) (Fig. 8). Cu, a common cofactor in methane cycling (Chi Fru et al., 2011; Glass and Orphan, 2012), in electron transport enzymes, oxidative stress protection, iron metabolism and connective tissue formation (Olivares and Uauy, 1996), is averagely more enriched in Franceville (EF = 0.88) compared to Burgess Shale (EF = 0.47), but is overall depleted in both deposits relative to PAAS (Fig. 8). Similarly, Co, vital primarily as a component of vitamin cobalamin (B_{12}), red blood cell formation, DNA synthesis and nitrogen fixation by supporting the activity of symbiotic nitrogen-fixing bacteria (Ma et al., 2021), is depleted in both Burgess and Franceville, with mean EF of 0.70 and 0.66, respectively (Fig. 8). V, important for biological activity in algae and microbial nitrogen fixation (Darnajoux et al., 2019), but non-essential for life forms (Liting et al., 2025), is homogeneously depleted in both the Burgess and Francevillian successions, recording mean EFs of 0.45 and 0.32, respectively (Fig. 8). Normalization of elemental concentrations to detrital proxies (Al and Ti) indicates that P, Fe, Co, Cu, Ni, and Zn in the Francevillian FB2b unit are less influenced by detrital input, but more so in the Burgess Shale (Fig. 6). In contrast, As, Mo, and V show a roughly equal contribution from detrital and non-detrital sources in both basins (Fig. 6e-f). Notably, Zn, Ni, and Cu display stronger non-detrital enrichment in FB2b than in the Burgess Shale (Fig. 6e-f), suggesting that these trace metal nutrients were more bioavailable in Francevillian seawater. As already noted, a coupling between elevated bioavailable Zn in FB2b and the emergence of eukaryotic macrofossils in the Francevillian Basin was previously reported by two separate groups of researchers (El Albani et al., 2023; Ossa Ossa et al., 2023).

As supported by existing geochemical compilations (e.g., Guilbaud, 2025; Lyons et al., 2014; Reinhard et al., 2017), elevated nutrient availability in the Paleoproterozoic was spatially and temporally heterogeneous, with sustained enrichments above PAAS not expected to be widespread. In this context, the magnitude of some PAAS-normalized nutrient enrichments observed in the Francevillian FB2b unit (including P, Zn and Ni) appears uncommon for sedimentary successions of this age, particularly under dominantly oxic depositional conditions. For instance, bulk sedimentary P levels underlying the FB2b subunit are reported to have reached concentrations that are rarely observed in sedimentary successions prior to the Ediacaran, but become more common in Ediacaran strata and throughout the Phanerozoic (Chi Fru et al., 2024). Although the present comparison focuses primarily on the Burgess Shale as a well-characterized post-oxygenation benchmark, broader evaluation against additional Precambrian black shale successions would further refine the assessment of how exceptional these enrichments were within the Paleoproterozoic record.

5. Conclusions

This comparative study of the Francevillian (Paleoproterozoic, ~2.1 Ga) and the Burgess Shales (Cambrian, ~508 Ma) offers valuable insights into the nutrient availability and redox conditions that prevailed during two critical biologically innovative windows in Earth's history. These formations, though separated by more than 1.5 billion years, both hosted exceptional biotas that are central to our understanding of early experimentation and eventual evolution of complex life, the former potentially representing some of the earliest multicellular macroorganisms, and the latter documenting the Cambrian explosion of metazoan diversity. Despite the vast temporal gap and differences in tectonic, depositional style, atmospheric and biological context, the geochemical results presented here reveal surprisingly convergent signatures in the provenance and enrichment levels of key bio-essential elements and redox-sensitive proxies. The data show that the Francevillian Basin was a remarkable Paleoproterozoic exception. Intense chemical weathering and inherited volcanic activity led to unprecedented seawater enrichment with P and Zn, both key nutrients for macrobiological evolution, along with elevated Ni, all at levels likely far above those present in the Burgess Shale ocean, celebrated for its animal biodiversity. Both basins record fully oxic bottom waters, indicating that these nutrient-rich conditions supported unusually high primary productivity that drove the deposition of the organic carbon–rich black shales that likely sustained the Francevillian macrobiota. Overall, the findings suggest that although Earth's atmosphere and oceans changed profoundly between the Paleoproterozoic and Cambrian, a restricted nutrient-rich environment like the Francevillian Basin may have already met some of the critical chemical and environmental prerequisites for macrobiological complexity, well before the end-Snowball Earth surge

in the seawater nutrient content that fueled the global Ediacaran–Cambrian rise of metazoans.

Author contributions

A.E.A. conceived and headed the project. A.E.K. and E.C.F. wrote the manuscript. A.E.K., E.C.F., C.A. and A.E.A. did the field work. A.E.K., I. C., M.H and A.E.A. prepared the samples. All authors discussed the results and reviewed the manuscript.

CRediT authorship contribution statement

Anna El Khoury: Writing – review & editing, Writing – original draft, Validation, Software, Methodology, Formal analysis, Data curation. **Ernest Chi Fru:** Writing – review & editing, Writing – original draft, Visualization, Validation, Resources, Methodology. **Ibtissam Chraiki:** Writing – review & editing, Validation, Methodology. **Mathias Harzhauser:** Writing – review & editing, Validation. **Christian Aupissy:** Writing – review & editing. **Claude Fontaine:** Writing – review & editing. **Andrea Somogyi:** Writing – review & editing. **Abderrazak El Albani:** Writing – review & editing, Writing – original draft, Visualization, Validation, Supervision, Resources, Methodology, Investigation, Funding acquisition, Formal analysis, Data curation, Conceptualization.

Declaration of competing interest

The authors declare that they have no known competing financial interests or personal relationships that could have appeared to influence the work reported in this paper.

Acknowledgements

We thank La Région Nouvelle Aquitaine (Project Darwin, grant E458CR25), the French government program “Investissements d'Avenir” (EUR INTREE, reference ANR-18-EURE-0010), the Synchrotron SOLEIL, ANR-BIOGEN, grant, 22-CE49-0010-02) and the European Research Council (ERC) Seventh Framework (F7) program, grant No: 336092 for their financial support. For the loan of Burgess fossils, we thank the Natural History Museum, Vienna. We also thank the CENAREST Gabonais, the COMILOG and SOCOBA Companies, the French Embassy in Libreville and the Institut Français du Gabon, for their support. We appreciate the technical and logistical help of C. Lebailly, A. Ngomanda, C. Laforest, A. Riboulleau, F. Baudin and R. Oslisly.

Appendix A. Supplementary data

Supplementary data to this article can be found online at https://doi.org/10.1016/j.precamres.2026.108064.

Data availability

Data will be made available on request.

References

Alcott, L.J., Mills, B.J.W., Bekker, A., Poulton, S.W., 2022. Earth’s great oxidation event facilitated by the rise of sedimentary phosphorus recycling. Nat. Geosci. 15, 210–215. https://doi.org/10.1038/s41561-022-00906-5.

Algeo, T.J., Liu, J., 2020. A re-assessment of elemental proxies for paleoredox analysis. Chem. Geol. 540, 119549. https://doi.org/10.1016/j.chemgeo.2020.119549.

Algeo, T.J., Maynard, J.B., 2004. Trace-element behavior and redox facies in core shales of Upper Pennsylvanian Kansas-type cyclothems. Chem. Geol. 206, 289–318. https://doi.org/10.1016/j.chemgeo.2003.12.009.

Anderson, R.P., Tosca, N.J., Saupe, E.E., Wade, J., Briggs, D.E.G., 2021. Early formation and taphonomic significance of kaolinite associated with Burgess Shale fossils. Geology 49, 355–359. https://doi.org/10.1130/G48067.1.

Anderson, T.B., James, M.J., McNeil, P., 2024. The Burgess Shale lagerstätte at the Walcott Quarry, Yoho National Park, Canada. SP 543, 77–84. https://doi.org/10.1144/SP543-2022-337.

Arnon, D.I., 1965. Ferredoxin and Photosynthesis: an iron-containing protein is a key factor in energy transfer during photosynthesis. Science 149, 1460–1470. https://doi.org/10.1126/science.149.3691.1460.

Aubineau, J., El Albani, A., Bekker, A., Chi Fru, E., Somogyi, A., Medjoubi, K., Riboulleau, A., Meunier, A., Konhauser, K.O., 2020. Trace element perspective into the ca. 2.1-billion-year-old shallow-marine microbial mats from the Francevillian Group, Gabon. Chem. Geol. 543, 119620. https://doi.org/10.1016/j.chemgeo.2020.119620.

Aubineau, J., El Albani, A., Bekker, A., Somogyi, A., Bankole, O.M., Macchiarelli, R., Meunier, A., Riboulleau, A., Reynaud, J.-Y., Konhauser, K.O., 2019. Microbially induced potassium enrichment in Paleoproterozoic shales and implications for reverse weathering on early Earth. Nat. Commun. 10, 2670. https://doi.org/10.1038/s41467-019-10620-3.

Aubineau, J., El Albani, A., Chi Fru, E., Gingras, M., Batonneau, Y., Buatois, L.A., Geffroy, C., Labanowski, J., Laforest, C., Lemée, L., Mángano, M.G., Meunier, A., Pierson-Wickmann, A.-C., Recourt, P., Riboulleau, A., Trentesaux, A., Konhauser, K. O., 2018. Unusual microbial mat-related structural diversity 2.1 billion years ago and implications for the Francevillian biota. Geobiology 16, 476–497. https://doi.org/10.1111/gbi.12296.

Babcock, L.E., Peng, S.-C., Brett, C.E., Zhu, M.-Y., Ahlberg, P., Bevis, M., Robison, R.A., 2015. Global climate, sea level cycles, and biotic events in the Cambrian Period. Palaeoworld 24, 5–15. https://doi.org/10.1016/j.palwor.2015.03.005.

Bankole, O.M., El Albani, A., Meunier, A., Gauthier-Lafaye, F., 2015. Textural and paleofluid flow control on diagenesis in the Paleoproterozoic Franceville Basin, South Eastern, Gabon. Precambr. Res. 268, 115–134. https://doi.org/10.1016/j.precamres.2015.07.008.

Bankole, O.M., El Albani, A., Meunier, A., Poujol, M., Bekker, A., 2020. Elemental geochemistry and Nd isotope constraints on the provenance of the basal siliciclastic succession of the middle Paleoproterozoic Francevillian Group. Gabon. Precambrian Research 348, 105874. https://doi.org/10.1016/j.precamres.2020.105874.

Behar, F., Beaumont, V., De B. Penteado, H.L., 2001. Rock-Eval 6 Technology: Performances and Developments. Oil & Gas Science and Technology - Rev. IFP 56, 111–134. Doi: 10.2516/ogst:2001013.

Bennett, W.W., Canfield, D.E., 2020. Redox-sensitive trace metals as paleoredox proxies: a review and analysis of data from modern sediments. Earth Sci. Rev. 204, 103175. https://doi.org/10.1016/j.earscirev.2020.103175.

Bertrand-Sarfati, J., Potin, B., 1994. Microfossiliferous cherty stromatolites in the 2000 Ma Franceville Group, Gabon. Precambr. Res. 65, 341–356. https://doi.org/10.1016/0301-9268(94)90112-0.

Boström, K., 1970. Submarine volcanism as a source for iron. Earth Planet. Sci. Lett. 9, 348–354. https://doi.org/10.1016/0012-821X(70)90134-2.

Bottjer, D.J. (Ed.), 2002. Exceptional Fossil Preservation: a Unique View on the Evolution of Marine Life, Critical Moments and Perspectives in Earth History and Paleobiology. Columbia Univ. Press, New York, NY.

Brocks, J.J., Jarrett, A.J.M., Sirantoine, E., Hallmann, C., Hoshino, Y., Liyanage, T., 2017. The rise of algae in Cryogenian oceans and the emergence of animals. Nature 548, 578–581. https://doi.org/10.1038/nature23457.

Bruland, K.W., Lohan, M.C., 2006. Controls of trace metals in seawater. Treatise on Geochemistry. 23–47.

Calvert, S.E., Pedersen, T.F., 1993. Geochemistry of recent oxic and anoxic marine sediments: Implications for the geological record. Mar. Geol. 113, 67–88. https://doi.org/10.1016/0025-3227(93)90150-T.

Canfield, D.E., Ngombi-Pemba, L., Hammarlund, E.U., Bengtson, S., Chaussidon, M., Gauthier-Lafaye, F., Meunier, A., Riboulleau, A., Rollion-Bard, C., Rouxel, O., Asael, D., Pierson-Wickmann, A.-C., El Albani, A., 2013. Oxygen dynamics in the aftermath of the great oxidation of earth’s atmosphere. PNAS 110, 16736–16741. https://doi.org/10.1073/pnas.1315570110.

Canfield, D.E., Poulton, S.W., Narbonne, G.M., 2007. Late-neoproterozoic deep-ocean oxygenation and the rise of animal life. Science 315, 92–95. https://doi.org/10.1126/science.1135013.

Carignan, J., Hild, P., Mevelle, G., Morel, J., Yeghicheyan, D., 2001. Routine analyses of trace elements in geological samples using flow injection and low pressure on-line liquid chromatography coupled to ICP-MS: a study of geochemical reference materials BR, DR-N, UB-N, AN-G and GH. Geostand. Newslett. 25, 187–198. https://doi.org/10.1111/j.1751-908X.2001.tb00595.x.

Caron, J.-B., Gaines, R.R., Aria, C., Mángano, M.G., Streng, M., 2014. A new phyllopod bed-like assemblage from the Burgess Shale of the Canadian Rockies. Nat. Commun. 5, 3210. https://doi.org/10.1038/ncomms4210.

Caron, J.-B., Jackson, D.A., 2008. Paleoecology of the greater phyllopod bed community, Burgess Shale. Palaeogeogr. Palaeoclimatol. Palaeoecol. 258, 222–256. https://doi.org/10.1016/j.palaeo.2007.05.023.

Chi Fru, E., Aubineau, J., Bankole, O., Ghnahalla, M., Tamehe, L.S., El Albani, A., 2024. Hydrothermal seawater eutrophication triggered local macrobiological experimentation in the 2100 Ma Paleoproterozoic Francevillian sub-basin. Precambr. Res. 409, 107453. https://doi.org/10.1016/j.precamres.2024.107453.

Chi Fru, E., Bahri, J.A., Brosson, C., Bankole, O., Aubineau, J., El Albani, A., Nederbragt; , A., Oldroyd, A., Skelton, A., Lowhagen, L., Webster, D., Fantong, W.Y., Mills, B.J. W., Alcott, L.J., Konhauser, K.O., Lyons, T.W., 2023. Transient fertilization of a post-Sturtian Snowball ocean margin with dissolved phosphate by clay minerals. Nat. Commun. 14, 8418. https://doi.org/10.1038/s41467-023-44240-9.

Chi Fru, E., Callac, N., Posth, N.R., Argyraki, A., Ling, Y.-C., Ivarsson, M., Broman, C., Kilias, S.P., 2018. Arsenic and high affinity phosphate uptake gene distribution in

shallow submarine hydrothermal sediments. Biogeochemistry 141, 41–62. https://doi.org/10.1007/s10533-018-0500-8.
Chi Fru, E., Gray, N.D., McCann, C., Baptista, J.D.C., Christgen, B., Talbot, H.M., El Ghazouani, A., Dennison, C., Graham, D.W., 2011. Effects of copper mineralogy and methanobactin on cell growth and sMMO activity in *Methylosinus trichosporium* OB3b. Biogeosciences 8, 2887–2894. https://doi.org/10.5194/bg-8-2887-2011.
Chi Fru, E., Hemmingsson, C., Holm, M., Chiu, B., Iñiguez, E., 2016. Arsenic-induced phosphate limitation under experimental Early Proterozoic oceanic conditions. Earth Planet. Sci. Lett. 434, 52–63. https://doi.org/10.1016/j.epsl.2015.11.009.
Chi Fru, E., Somogyi, A., El Albani, A., Medjoubi, K., Aubineau, J., Robbins, L.J., Lalonde, S.V., Konhauser, K.O., 2019. The rise of oxygen-driven arsenic cycling at ca. 2.48 Ga. Geology 47, 243–246. https://doi.org/10.1130/G45676.1.
Chraiki, I., Chi Fru, E., Somogyi, A., Bouougri, E.H., Bankole, O., Ghnahalla, M., El Albani, A., 2023. Blooming of a microbial community in an Ediacaran extreme volcanic lake system. Sci. Rep. 13, 9080. https://doi.org/10.1038/s41598-023-36031-5.
Clarkson, M.O., Poulton, S.W., Guilbaud, R., Wood, R.A., 2014. Assessing the utility of Fe/Al and Fe-speciation to record water column redox conditions in carbonate-rich sediments. Chem. Geol. 382, 111–122. https://doi.org/10.1016/j.chemgeo.2014.05.031.
Collins, D.H., Briggs, D., Morris, S.C., 1983. New Burgess Shale fossil sites reveal middle Cambrian faunal complex. Science 222, 163–167.
Collom, C.J., Johnston, P.A., Powell, W.G., 2009. Reinterpretation of 'Middle' Cambrian stratigraphy of the rifted western Laurentian margin: burgess shale formation and contiguous units (Sauk II megasequence), Rocky Mountains, Canada. Palaeogeogr. Palaeoclimatol. Palaeoecol. 277, 63–85. https://doi.org/10.1016/j.palaeo.2009.02.012.
Darnajoux, R., Magain, N., Renaudin, M., Lutzoni, F., Bellenger, J.-P., Zhang, X., 2019. Molybdenum threshold for ecosystem scale alternative vanadium nitrogenase activity in boreal forests. PNAS 116, 24682–24688. https://doi.org/10.1073/pnas.1913314116.
El Albani, A., Bengtson, S., Canfield, D.E., Bekker, A., Macchiarelli, R., Mazurier, A., Hammarlund, E.U., Boulvais, P., Dupuy, J.-J., Fontaine, C., Fürsich, F.T., Gauthier-Lafaye, F., Janvier, P., Javaux, E., Ossa, F.O., Pierson-Wickmann, A.-C., Riboulleau, A., Sardini, P., Vachard, D., Whitehouse, M., Meunier, A., 2010. Large colonial organisms with coordinated growth in oxygenated environments 2.1 Gyr ago. Nature 466, 100–104. https://doi.org/10.1038/nature09166.
El Albani, A., Bengtson, S., Canfield, D.E., Riboulleau, A., Rollion Bard, C., Macchiarelli, R., Ngombi Pemba, L., Hammarlund, E., Meunier, A., Moubiya Mouele, I., Benzerara, K., Bernard, S., Boulvais, P., Chaussidon, M., Cesari, C., Fontaine, C., Chi-Fru, E., Garcia Ruiz, J.M., Gauthier-Lafaye, F., Mazurier, A., Pierson-Wickmann, A.C., Rouxel, O., Trentesaux, A., Vecoli, M., Versteegh, G.J.M., White, L., Whitehouse, M., Bekker, A., 2014. The 2.1 Ga old francevillian biota: biogenicity, taphonomy and biodiversity. PLoS One 9, e99438. https://doi.org/10.1371/journal.pone.0099438.
El Albani, A., Konhauser, K.O., Somogyi, A., Ngwalghoubou Ikouanga, J., Lamboux, A., Blichert-Toft, J., Chi-Fru, E., Fontaine, C., Mazurier, A., Riboulleau, A., Pierson-Wickmann, A.-C., Albarède, F., 2023. A search for life in Palaeoproterozoic marine sediments using Zn isotopes and geochemistry. Earth Planet. Sci. Lett. 612, 118169. https://doi.org/10.1016/j.epsl.2023.118169.
El Albani, A., Mangano, M.G., Buatois, L.A., Bengtson, S., Riboulleau, A., Bekker, A., Konhauser, K., Lyons, T., Rollion-Bard, C., Bankole, O., Lekele Baghekema, S.G., Meunier, A., Trentesaux, A., Mazurier, A., Aubineau, J., Laforest, C., Fontaine, C., Recourt, P., Chi Fru, E., Macchiarelli, R., Reynaud, J.Y., Gauthier-Lafaye, F., Canfield, D.E., 2019. Organism motility in an oxygenated shallow-marine environment 2.1 billion years ago. PNAS 116, 3431–3436. https://doi.org/10.1073/pnas.1815721116.
El Khoury, A., Chraiki, I., Fontaine, C., Somogyi, A., El Albani, A., 2025a. Paleosalinity reconstruction of the Francevillian Basin (2.1 Ga): geochemical insights into the depositional environment of early macroscopic life. Comptes Rendus. Géoscience 357, 557–587. https://doi.org/10.5802/crgeos.319.
El Khoury, A., Saleh, F., El Albani, A., Fontaine, C., Rollion-Bard, C., Chraiki, I., Aubineau, J., Ngwal'ghoubou Ikouanga, J., Bhilisse, M., Zguaid, M., Somogyi, A., Chi Fru, E., 2025b. Pyrite morphology and sulfur isotopes refine taphonomic models for the 2.1 Ga Francevillian biota, Gabon. Sci Rep 15, 19790. Doi: 10.1038/s41598-025-04512-4.
El Khoury, A., Somogyi, A., Chi Fru, E., Saleh, F., Chraiki, I., Fontaine, C., Aubineau, J., Rollion-Bard, C., Harzhauser, M., El Albani, A., 2025c. A battle against arsenic toxicity by Earth's earliest complex life forms. Nat. Commun. 16, 4388. https://doi.org/10.1038/s41467-025-59760-9.
Elias, M., Wellner, A., Goldin-Azulay, K., Chabriere, E., Vorholt, J.A., Erb, T.J., Tawfik, D. S., 2012. The molecular basis of phosphate discrimination in arsenate-rich environments. Nature 491, 134–137. https://doi.org/10.1038/nature11517.
Falkowski, P.G., Fenchel, T., Delong, E.F., 2008. The microbial engines that drive earth's biogeochemical cycles. Science 320, 1034–1039. https://doi.org/10.1126/science.1153213.
Fedo, C., 1995. Unraveling the effects of potassium metasomatism in sedimentary rocks and paleosols, with implications for paleoweathering conditions and provenance.
Fletcher, T.P., Collins, D.H., 1998. The Middle Cambrian Burgess Shale and its relationship to the Stephen Formation in the southern Canadian Rocky Mountains 35.
Gaines, R.R., Briggs, D.E.G., Yuanlong, Z., 2008. Cambrian burgess shale–type deposits share a common mode of fossilization. Geol 36, 755. https://doi.org/10.1130/G24961A.1.
Gauthier-Lafaye, F., Holliger, P., Blanc, P.-L., 1996. Natural fission reactors in the Franceville basin, Gabon: a review of the conditions and results of a "critical event" in a geologic system. Geochim. Cosmochim. Acta 60, 4831–4852. https://doi.org/10.1016/S0016-7037(96)00245-1.
Gauthier-Lafaye, F., Weber, F., 1989. The Francevillian (lower Proterozoic) uranium ore deposits of Gabon. Econ. Geol. 84, 2267–2285. https://doi.org/10.2113/gsecongeo.84.8.2267.
Glass, J.B., Orphan, V.J., 2012. Trace metal requirements for microbial enzymes involved in the production and consumption of methane and nitrous oxide. Front. Microbio. 3. https://doi.org/10.3389/fmicb.2012.00061.
Guilbaud, R., 2025. Proterozoic evolution of the phosphorus cycle: Was it high or was it low?, in: Treatise on Geochemistry. Elsevier, pp. 153–175. Doi: 10.1016/B978-0-323-99762-1.00068-1.
Harasim, P., Filipek, T., Harasim, P., 2015. Nickel in the environment. J. Elem. https://doi.org/10.5601/jelem.2014.19.3.651.
Harnois, L., 1988. The CIW index: a new chemical index of weathering. Sed. Geol. 55, 319–322. https://doi.org/10.1016/0037-0738(88)90137-6.
Hoffman, P.F., Abbot, D.S., Ashkenazy, Y., Benn, D.I., Brocks, J.J., Cohen, P.A., Cox, G. M., Creveling, J.R., Donnadieu, Y., Erwin, D.H., Fairchild, I.J., Ferreira, D., Goodman, J.C., Halverson, G.P., Jansen, M.F., Le Hir, G., Love, G.D., Macdonald, F. A., Maloof, A.C., Partin, C.A., Ramstein, G., Rose, B.E.J., Rose, C.V., Sadler, P.M., Tziperman, E., Voigt;, A., Warren, S.G., 2017. Snowball Earth climate dynamics and Cryogenian geology-geobiology. Sci. Adv. 3, e1600983. https://doi.org/10.1126/sciadv.1600983.
Ikouanga, J.N., Fontaine, C., Bourdelle, F., Abd Elmola, A., Aubineau, J., Bankole, O.M., Reisberg, L., Pierson-Wickmann, A.-C., Riboulleau, A., Trentesaux, A., Laforest, C., Meunier, A., El Albani, A., 2023. Taphonomy of early life (2.1 Ga) in the francevillian basin (Gabon): role of organic mineral interactions. Precambr. Res. 395, 107155. https://doi.org/10.1016/j.precamres.2023.107155.
Ikouanga, J.N., Reisberg, L., Pierson-Wickmann, A.-C., El Khoury, A., Fontaine, C., El Albani, A., 2024. The first application of Re–Os dating on Paleoproterozoic Francevillian sediments (Gabon). Comptes. Rendus. Géosci. 356, 57–66. https://doi.org/10.5802/crgeos.264.
Jiang, L., Zhao, M., Shen, A., Huang, L., Chen, D., Cai, C., 2022. Pulses of atmosphere oxygenation during the Cambrian radiation of animals. Earth Planet. Sci. Lett. 590, 117565. https://doi.org/10.1016/j.epsl.2022.117565.
Jones, B., Manning, D.A.C., 1994. Comparison of geochemical indices used for the interpretation of palaeoredox conditions in ancient mudstones. Chem. Geol. 111, 111–129. https://doi.org/10.1016/0009-2541(94)90085-X.
Kimura, H., Watanabe, Y., 2001. Oceanic anoxia at the Precambrian-Cambrian boundary. Geol 29, 995. https://doi.org/10.1130/0091-7613(2001).
Korenaga, J., 2013. Initiation and evolution of plate tectonics on earth: theories and observations. Annu. Rev. Earth Planet. Sci. https://doi.org/10.1146/annurev-earth-050212-124208.
Kustka, A., Carpenter, E.J., Sañudo-Wilhelmy, S.A., 2002. Iron and marine nitrogen fixation: progress and future directions. Res. Microbiol. 153, 255–262. https://doi.org/10.1016/S0923-2508(02)01325-6.
Laakso, T.A., Sperling, E.A., Johnston, D.T., Knoll, A.H., 2020. Ediacaran reorganization of the marine phosphorus cycle. PNAS 117, 11961–11967. https://doi.org/10.1073/pnas.1916738117.
Lawrence, M.G., Greig, A., Collerson, K.D., Kamber, B.S., 2006. Rare earth element and yttrium variability in South East Queensland Waterways. Aquat. Geochem. 12, 39–72. https://doi.org/10.1007/s10498-005-4471-8.
Lawrence, M.G., Kamber, B.S., 2006. The behaviour of the rare earth elements during estuarine mixing—revisited. Mar. Chem. 100, 147–161. https://doi.org/10.1016/j.marchem.2005.11.007.
Lee, C.-T.-A., Yeung, L.Y., McKenzie, N.R., Yokoyama, Y., Ozaki, K., Lenardic, A., 2016. Two-step rise of atmospheric oxygen linked to the growth of continents. Nat. Geosci. 9, 417–424. https://doi.org/10.1038/ngeo2707.
Lentz, D.R., 2003. Geochemistry of sediments and sedimentary rocks: historical to research perspectives.
Lim, N.C., Freake, H.C., Brückner, C., 2005. Illuminating Zinc in Biological Systems. Chem. A Eur. J. 11, 38–49. https://doi.org/10.1002/chem.200400599.
Liting, H., Siling, R., Litian, W., Bin, J., Jixiang, W., Ranbin, L., Xiaodi, H., 2025. Application of settleable algae in vanadium(V) removal and the response mechanisms. J. Environ. Chem. Eng. 13, 116094. https://doi.org/10.1016/j.jece.2025.116094.
Liu, J., Algeo, T.J., 2020. Beyond redox: Control of trace-metal enrichment in anoxic marine facies by watermass chemistry and sedimentation rate. Geochim. Cosmochim. Acta 287, 296–317. https://doi.org/10.1016/j.gca.2020.02.037.
Liu, L., Gurnis, M., Seton, M., Saleeby, J., Müller, R.D., Jackson, J.M., 2010. The role of oceanic plateau subduction in the Laramide orogeny. Nature Geosci. 3, 353–357. https://doi.org/10.1038/ngeo829.
Lyons, T., Reinhard, C., Planavsky, N., 2014. The rise of oxygen in Earth's early ocean and atmosphere.
Lyons, T.W., Severmann, S., 2006. A critical look at iron paleoredox proxies: new insights from modern euxinic marine basins. Geochim. Cosmochim. Acta 70, 5698–5722. https://doi.org/10.1016/j.gca.2006.08.021.
Lyons, T.W., Tino, C.J., Fournier, G.P., Anderson, R.E., Leavitt, W.D., Konhauser, K.O., Stüeken, E.E., 2024. Co-evolution of early Earth environments and microbial life. Nat. Rev. Microbiol. 22, 572–586. https://doi.org/10.1038/s41579-024-01044-y.
Ma, J., Song, Z., Yang, J., Wang, Y., Han, H., 2021. Cobalt ferrite nanozyme for efficient symbiotic nitrogen fixation *via* regulating reactive oxygen metabolism. Environ. Sci. Nano 8, 188–203. https://doi.org/10.1039/d0en00935k.
Ma, X., Edgecombe, G.D., Hou, X., Goral, T., Strausfeld, N.J., 2015. Preservational pathways of corresponding Brains of a Cambrian Euarthropod. Curr. Biol. 25, 2969–2975. https://doi.org/10.1016/j.cub.2015.09.063.

Marshall, C.R., 2006. Explaining the cambrian “explosion” of animals. Annu. Rev. Earth Planet. Sci. 34, 355–384. https://doi.org/10.1146/annurev.earth.33.031504.103001.
Marynowski, L., Zatoń, M., Rakociński, M., Filipiak, P., Kurkiewicz, S., Pearce, T.J., 2012. Deciphering the upper Famennian Hangenberg Black Shale depositional environments based on multi-proxy record. Palaeogeogr. Palaeoclimatol. Palaeoecol. 346–347, 66–86. https://doi.org/10.1016/j.palaeo.2012.05.020.
Mayika, K.B., Moussavou, M., Prave, A.R., Lepland, A., Mbina, M., Kirsimäe, K., 2020. The Paleoproterozoic Francevillian succession of Gabon and the Lomagundi-Jatuli event. Geology 48, 1099–1104. https://doi.org/10.1130/G47651.1.
Herron, M.M., 1988. Geochemical classification of terrigenous sands and shales from core or log data. SEPM JSR 58. https://doi.org/10.1306/212F8E77-2B24-11D7-8648000102C1865D.
Moore, D.M., Reynolds, R.C., 1997. X-ray Diffraction and the Identification and Analysis of Clay Minerals.
Morris, S.C., 1989. Burgess Shale Faunas and the Cambrian Explosion. Science 246, 339–346. https://doi.org/10.1126/science.246.4928.339.
Narbonne, G.M., 2005. THE EDIACARA BIOTA: neoproterozoic origin of animals and their ecosystems. Annu. Rev. Earth Planet. Sci. 33, 421–442. https://doi.org/10.1146/annurev.earth.33.092203.122519.
Nesbitt, H.W., Young, G.M., 1982. Early Proterozoic climates and plate motions inferred from major element chemistry of lutites. Nature 299.
Nesbitt, S.W., Zipser, E.J., 2003. The diurnal cycle of rainfall and convective intensity according to three years of TRMM measurements. J. Clim. 16.
Ngombi-Pemba, L., Albani, A.E., Meunier, A., Grauby, O., Gauthier-Lafaye, F., 2014. From detrital heritage to diagenetic transformations, the message of clay minerals contained within shales of the Palaeoproterozoic Francevillian basin (Gabon). Precambr. Res. 255, 63–76. https://doi.org/10.1016/j.precamres.2014.09.016.
Och, L.M., Shields-Zhou, G.A., 2012. The Neoproterozoic oxygenation event: environmental perturbations and biogeochemical cycling. Earth Sci. Rev. 110, 26–57. https://doi.org/10.1016/j.earscirev.2011.09.004.
Olivares, M., Uauy, R., 1996. Copper as an essential nutrient. Am. J. Clin. Nutr. 63, 791S–S796. https://doi.org/10.1093/ajcn/63.5.791.
Orr, P.J., Briggs, D.E.G., Kearns, S.L., 1998. Cambrian burgess shale animals replicated in clay minerals. Science 281, 1173–1175. https://doi.org/10.1126/science.281.5380.1173.
Ossa Ossa, F., Pons, M.-L., Bekker, A., Hofmann, A., Poulton, S.W., Andersen, M.B., Agangi, A., Gregory, D., Reinke, C., Steinhilber, B., Marin-Carbonne, J., Schoenberg, R., 2023. Zinc enrichment and isotopic fractionation in a marine habitat of the c. 2.1 Ga Francevillian Group: a signature of zinc utilization by eukaryotes? Earth Planet. Sci. Lett. 611, 118147. https://doi.org/10.1016/j.epsl.2023.118147.
Pecoits, E., Gingras, M.K., Barley, M.E., Kappler, A., Posth, N.R., Konhauser, K.O., 2009. Petrography and geochemistry of the Dales Gorge banded iron formation: paragenetic sequence, source and implications for palaeo-ocean chemistry. Precambr. Res. 172, 163–187. https://doi.org/10.1016/j.precamres.2009.03.014.
Planavsky, N., Bekker, A., Rouxel, O.J., Kamber, B., Hofmann, A., Knudsen, A., Lyons, T. W., 2010. Rare earth element and yttrium compositions of Archean and Paleoproterozoic Fe formations revisited: new perspectives on the significance and mechanisms of deposition. Geochim. Cosmochim. Acta 74, 6387–6405. https://doi.org/10.1016/j.gca.2010.07.021.
Poulton, S.W., Bekker, A., Cumming, V.M., Zerkle, A.L., Canfield, D.E., Johnston, D.T., 2021. A 200-million-year delay in permanent atmospheric oxygenation. Nature 592, 232–236. https://doi.org/10.1038/s41586-021-03393-7.
Powell, W., 2009. Comparison of geochemical and distinctive mineralogical features associated with the Kinzers and Burgess Shale formations and their associated units. Palaeogeogr. Palaeoclimatol. Palaeoecol. 277, 127–140. https://doi.org/10.1016/j.palaeo.2009.02.016.
Powell, W.G., Johnston, P.A., Collom, C.J., 2003. Geochemical evidence for oxygenated bottom waters during deposition of fossiliferous strata of the Burgess Shale Formation. Palaeogeogr. Palaeoclimatol. Palaeoecol. 201, 249–268. https://doi.org/10.1016/S0031-0182(03)00612-6.
Pruss, S.B., Gill, B.C., 2024. Life on the edge: the cambrian marine realm and oxygenation. Annu. Rev. Earth Planet. Sci. 52, 109–132. https://doi.org/10.1146/annurev-earth-031621-070316.
Raiswell, R., Hardisty, D.S., Lyons, T.W., Canfield, D.E., Owens, J.D., Planavsky, N.J., Poulton, S.W., Reinhard, C.T., 2018. The iron paleoredox proxies: a guide to the pitfalls, problems and proper practice. Am. J. Sci. 318, 491–526. https://doi.org/10.2475/05.2018.03.
Reinhard, C.T., Planavsky, N.J., Gill, B.C., Ozaki, K., Robbins, L.J., Lyons, T.W., Fischer, W.W., Wang, C., Cole, D.B., Konhauser, K.O., 2017. Evolution of the global phosphorus cycle. Nature 541, 386–389. https://doi.org/10.1038/nature20772.
Reynaud, J.-Y., Trentesaux, A., El Albani, A., Aubineau, J., Ngombi-Pemba, L., Guiyeligou, G., Bouton, P., Gauthier-Lafaye, F., Weber, F., 2018. Depositional setting of the 2·1 Ga Francevillian macrobiota (Gabon): rapid mud settling in a shallow basin swept by high-density sand flows. Sedimentology 65, 670–701. https://doi.org/10.1111/sed.12398.
Salminen, J.M., Evans, D.A.D., Trindade, R.I.F., Oliveira, E.P., Piispa, E.J., Smirnov, A.V., 2016. Paleogeography of the Congo/São Francisco craton at 1.5Ga: expanding the core of Nuna supercontinent. Precambr. Res. 286, 195–212. https://doi.org/10.1016/j.precamres.2016.09.011.
Scotese, C.R., 2021. An Atlas of Phanerozoic Paleogeographic Maps: the Seas come In and the Seas Go out. Annu. Rev. Earth Planet. Sci. 49, 679–728. https://doi.org/10.1146/annurev-earth-081320-064052.
Singh, D., Khare, A., Singh, S., 2017. Effect of phosphorus and molybdenum nutrition on yield and nutrient uptake in lentil (Lens culinaris L.).
Stewart, W.D., Dixon, O.A., Rustt, B.R., 1993. Middle Cambrian carbonate-platform collapse, southeastern Canadian Rocky Mountains. Geol 21, 687. https://doi.org/10.1130/0091-7613(1993)021%253C0687:MCCPCS%253E2.3.CO;2.
Stüeken, E.E., Kipp, M.A., Koehler, M.C., Buick, R., 2016. The evolution of Earth’s biogeochemical nitrogen cycle. Earth Sci. Rev. 160, 220–239. https://doi.org/10.1016/j.earscirev.2016.07.007.
Sumner, D.Y., 2024. Oxygenation of Earth’s atmosphere induced metabolic and ecologic transformations recorded in the Lomagundi-Jatuli carbon isotopic excursion. Appl. Environ. Microbiol. 90, e00093–e00124. https://doi.org/10.1128/aem.00093-24.
Sun, S., Chen, A., Hou, M., Yang, S., Ogg, J.G., Zou, H., Xu, S., Li, Q., Huang, Y., Li, R., Chen, H., 2022. Rapid climatic fluctuations during the Guadalupian-Lopingian transition: implications from weathering indices recorded in acid-insoluble residues of carbonate rocks, South China. J. Asian Earth Sci. 230, 105222. https://doi.org/10.1016/j.jseaes.2022.105222.
Taylor, S.R., McLennan, S.M., 1985. The continental crust: its composition and evolution.
Tostevin, R., Shields, G.A., Tarbuck, G.M., He, T., Clarkson, M.O., Wood, R.A., 2016. Effective use of cerium anomalies as a redox proxy in carbonate-dominated marine settings. Chem. Geol. 438, 146–162. https://doi.org/10.1016/j.chemgeo.2016.06.027.
Tribovillard, N., Algeo, T.J., Lyons, T., Riboulleau, A., 2006. Trace metals as paleoredox and paleoproductivity proxies: an update. Chem. Geol. 232, 12–32. https://doi.org/10.1016/j.chemgeo.2006.02.012.
Wang, C., Dong, T., He, Z., Guo, X., Liu, S., 2024. Hydrographic restriction conditions in the Middle and Upper Yangtze region during the Early Silurian post-glacial transgression: constraints from major, trace elemental geochemistry and Mo-TOC relationship. Palaeogeogr. Palaeoclimatol. Palaeoecol. 655, 112546. https://doi.org/10.1016/j.palaeo.2024.112546.
Wang, P., Du, Y., Yu, W., Algeo, T.J., Zhou, Q., Xu, Y., Qi, L., Yuan, L., Pan, W., 2020. The chemical index of alteration (CIA) as a proxy for climate change during glacial-interglacial transitions in Earth history. Earth Sci. Rev. 201, 103032. https://doi.org/10.1016/j.earscirev.2019.103032.
Weber, F., 1968. Sédimentologie, géochiimie, relations avec les gites minéraux associés.
Weber, T., John, S., Tagliabue, A., DeVries, T., 2018. Biological uptake and reversible scavenging of zinc in the global ocean. Science 361, 72–76. https://doi.org/10.1126/science.aap8532.